Indian Journal of Pure & Applied Physics
Vol. 63, September 2025, pp. 859-865
DOI: 10.56042/ijpap.v63i9.20483

Fabrication of ZnO Thin Film Sensor using Sputtering for Low-level NO_2 detection

Pooja[a], Rita Dahiya[a], Annu Sheokand[a], Mamta Bulla[a], Sarita Sindhu[a], Poonam Rani[a], Kiran Jeet[b] & Vinay Kumar[a*]

[a]Department of Physics, CCS Haryana Agricultural University, Hisar, Haryana 125 004, India

[b]Electron Microscopy and Nanoscience Laboratory, Punjab Agricultural University, Ludhiana, Punjab 141 027, India

Received: 9th June 2025; accepted: 10th July 2025

The accurate detection and monitoring of gas levels in real-world environmental conditions remain a significant challenge. Gas sensing technologies are essential for detecting hazardous analytes such as NO_2, SO_2, CO, NH_3 and H_2S. Among these, detecting NO_2 at significant levels continues to pose a challenge. In this context, the present study investigates sputtering-based ZnO thin film gas sensors for the real-time detection of NO_2. The fabricated films were characterized to assess their structural, morphological, functional group, optical, and gas sensing properties using techniques such as XRD, FE-SEM, FTIR, PL and the Keithley 2450 Source Meter, respectively. The sensing analysis demonstrated the excellent performance of the fabricated film for NO_2 detection, with an optimum operating temperature of 200°C, achieving a 52% response at a concentration of 200 parts per million (ppm), along with a sensing response time of 44 seconds and a recovery time of 530 seconds. Furthermore, the sensor exhibited a detection limit as low as 43 ppb. The findings of this research underscore the significant potential of sputtered ZnO thin films as reliable and versatile candidates for advanced gas sensing technologies, paving the way for further innovations in environmental monitoring and safety applications.

Keywords: Thin film, Sputtering technique, Gas sensing, Environmental protection

1 Introduction

Gas sensor play a significant role in real world applications as the rapid industrialization and modernization processes release harmful gases into the atmosphere, such as nitrogen dioxide (NO_2), carbon dioxide (CO_2), hydrogen sulfide (H_2S), hydrogen (H_2), formaldehyde (HCHO), methane (CH_4), ammonia (NH_3), acetylene (C_2H_2) and volatile organic compounds (VOCs) like benzene, toluene, acetone, etc.[1,2,3]. Amongst all the pollutant gases, NO_2 shows adverse effects on human life and the ecosystem. This poisonous gas is released from industrial activities, emissions from automobiles, fossil fuel burning, etc., causing numerous negative effects on people's health, such as respiratory disease, brain stroke, and also contributing to ozone and acid rain formation[4,5]. Even a ppb level exposure of NO_2 for long period can raises severe adverse effects such as pneumonia, asthma, hay fever, damage to respiratory tract and eyes. According to National Institutes of Occupational Safety and Health (NIOSH), the short-term exposure limit of NO_2 is 1 ppm. Occupational Safety and Health Administration (OSHA) permissible limit is 5 ppm averaged over an 8-hour workday. The experimental studies showed that the long-term exposure of even low concentration of NO_2 (0.04 to 1.0 ppm) causes sub chronic and chronic effects on animals. The high concentration (8 to 25 ppm) exposure of the gas result in serious effects such as emphysema-like damage, airway hyper responsiveness and allergic-type immune responses. As a result, the detection of NO_2 gas becomes a priority for environmental and human safety[6,7,8]. Sensing technologies play a pivotal role in identifying hazardous gases and measuring their concentration levels in the environment. The gas sensing performance is greatly affected by the materials used in their fabrication[9, 10]. Among various materials opted for effective detection, metal oxides (ZnO, CuO, TiO_2, SnO_2, etc.) are widely researched and refined due to their excellent physical and chemical properties, thermal stability, availability, small size, affordability and suitability for many electronic devices. These materials are highly effective in detecting a wide range of gases, making them indispensable for sensor technology[11, 12].

ZnO is a transition metal oxide with excellent electrical, optical and mechanical properties. Two-dimensional ZnO nanostructures have shown considerable interest for their gas sensing properties due to their wide energy band gap value (3.10-3.40 eV), excellent thermal conductivity (approx. 50

*Corresponding author: E-mail: vinay23@hau.ac.in

W/mK) and surface area, better excitonic binding energy (approx. 60 meV), non-toxic and environment friendly nature. These properties make ZnO a superior material in real field applications, including optical detectors, LEDs, gas sensors, photovoltaic cells, and photocatalysis[13, 14]. Also, ZnO forms a variety of nanostructures, such as in one dimension (nanowires, nanotubes, nanorods, nanoribbons, nano springs, nanobelts, etc.), in two dimensions (nano pellets, nanosheet, etc.) and in three dimensions (nanoflower, nanoflakes, etc.). These different morphologies significantly affect the role of ZnO for one or other application[15].

This study highlighted the performance of ZnO thin film for gas sensing applications. For the fabrication of film, DC magnetron sputtering, a physical vapor deposition (PVD) technique, was used. In this technique, a ZnO target was inserted in the vacuum chamber and the desired substrates were attached to the substrate holder. The chamber was capable of achieving a vacuum of the order of 10^{-6} mbar. The electric field generated due to the potential difference between the target and the substrate holder provides the movement of free electrons towards the anode (or substrate). During the drifting of these electrons, the ionization of the sputtering gas (i.e., Ar gas) is carried out, resulting in the creation of Ar^+ gas ions. This collision of electrons with the sputtering gas further causes an avalanche effect. The movement of these Ar^+ ions towards the target generated plasma gas over there or maybe plasma ions over there. These high-energy plasma ions then strike the target surface, eject the surface atoms and then the deposition of these atoms is processed onto the surface of substrate, resulting in the film's fabrication[18,19]. The whole process of ZnO film deposition is illustrated in Fig. 1.

2 Experimental Details

The DC magnetron sputtering method was adopted for the fabrication of ZnO nano structured thin films. A solid target of Zn metal (50.8 mm in diameter and 5 mm in thickness) is utilized for sputtering process. The substrate to target distance was kept 10 cm and the substrate temperature was maintained at room temperature (~25 °C). The substrates used were glass slides, cut in the dimensions of 1×1 cm^2. These substrates were cleaned using ultrasonicator for 10 minutes, subsequently with acetone and distilled water and then oven dried for 60 minutes at 80 °C. When they acquired room temperature then these were loaded on the substrate holder and placed in a vacuum chamber. The chamber was evacuated to base pressure of the order of 10^{-6} mbar. After evacuating the chamber, the sputtering gas (Ar, 20 sccm) was inserted and the plasma was created by maintaining a working pressure of about 4.4×10^{-3} mbar. The film was deposited at 25 W for a deposition time of 40 minutes with Ar:O_2 flow rate in the ratio of 20:2. After the successful fabrication of the film, it was calcinated for 2 hours at 400 °C. A thin layer of silver paste was applied on the film to provide contact support between the electrode and film and sensing parameters were noted.

3 Results and Discussion

The fabricated film was characterized by employing various techniques. X-ray Diffraction (XRD), Field Emission Scanning Electron Microscope (FE-SEM), Fourier Transform Infrared

(FTIR) and Photoluminescence (PL) studies were carried out to obtain structural information, surface characteristics, vibrational modes and the optical bandgap value of the prepared film, respectively.

Figure 2(a) represents the XRD spectra of ZnO nanostructured thin film corresponding to (002) and (103) planes at diffraction angles 34.16° and 62.32°, respectively. The sharp and most intense peak was obtained for the plane (002) corresponding to the angle of 34.16°, indicating the crystalline nature of the film. The XRD results revealed the wurtzite structure of the prepared film.The crystallite size was 5.9 nm, calculated using Debye-Scherrer' Eq. (1),

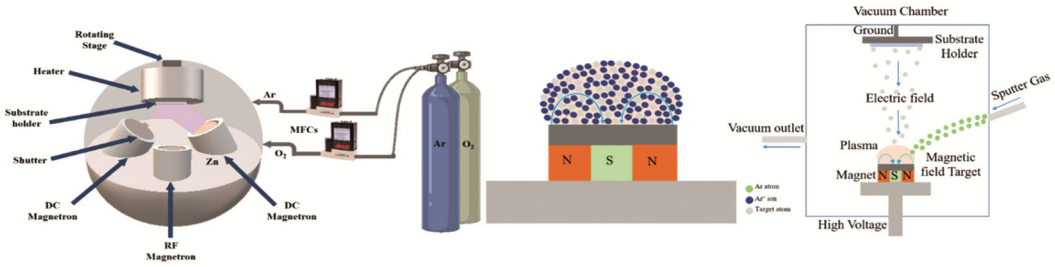

Fig. 1 — Schematic representation of Sputtering for the fabrication of ZnO thin film

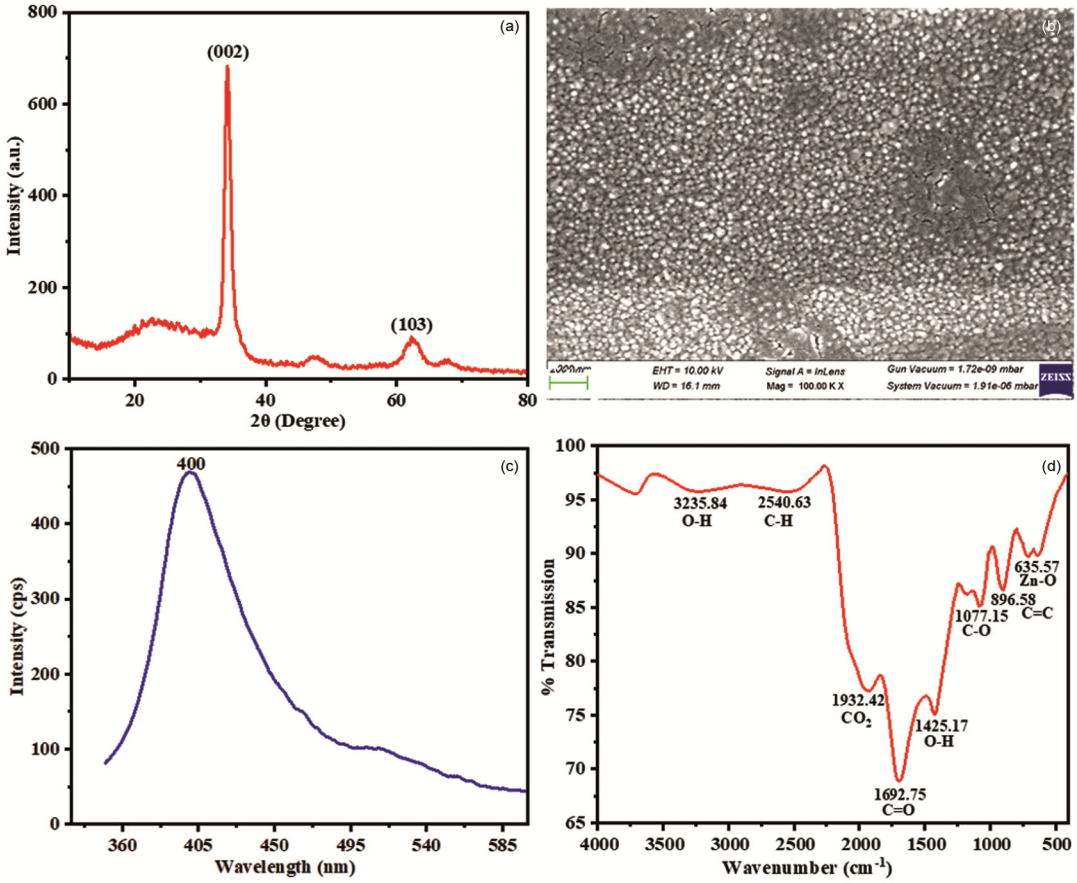

Fig. 2 — (a) X-ray diffraction pattern (b) FE-SEM micrograph (c) PL emission spectrum and (d) FTIR spectrum of ZnO film

$$d = \frac{k\lambda}{\beta cos\theta} \quad \ldots (1)$$

where, k is a numerical constant (=0.9), λ is the incident radiation wave length (i.e., λ(Cu K_α) = 1.54 Å) and β represents to full width half maxima (FWHM) of the most intense diffraction peak appearing at angle 2θ.

The morphology of thin film was analyzed by FE-SEM (Fig. 2(b)). The SEM image shows that the surface of the prepared film is smooth, indicating the uniformly distributed grains throughout the surface of the film, important for the good sensing properties. The optical bandgap value was calculated by using PL spectroscopy. The measurement was performed by taking320 nm as the excitation wavelength. The absorption peak at a wavelength of 400 nm is observed for the fabricated ZnO film as shown in Fig. 2(c). The calculated bandgap value of the film was 3.1 eV, which showed the semiconducting nature of ZnO film.

Fig. 2(d) represents the FTIR spectrum for the developed film in the range of 4000-400 cm^{-1}. The different peaks observed in FTIR spectrum indicate the different vibrations or stretching or bending present in the ZnO film. The peak at 635.57 cm^{-1} indicates the presence of Zn-O bond[20,21]. Additionally, the peak observed at 3235.84 cm^{-1}, 2540.63 cm^{-1}, 1932.42 cm^{-1}, 1692.75 cm^{-1}, 1425.17 cm^{-1}, 1077.15 cm^{-1} and 896.58 cm^{-1} ascribed to O-H, C-H, CO_2, C=O, O-H, C-O, C=C group, respectively, which may be due to the presence of moisture and impurities in the sample under study.

4 Sensing Analysis

The gas sensing parameters of the film was evaluated using chemiresistive gas sensor, which comprises of stainless-steel chamber having volume of 200 cm^3 and equipped with one circular heater. All the sensing analysis were performed using two probe method via Keithley 2450 source meter. The heater surface is used as a sample holder and the electrodes were connected to the sample through the thin layer of silver paste applied on the opposite corner of the film. For sensing analysis, the mixed ratio of air and gas analyte was inserted in the chamber with a flow rate

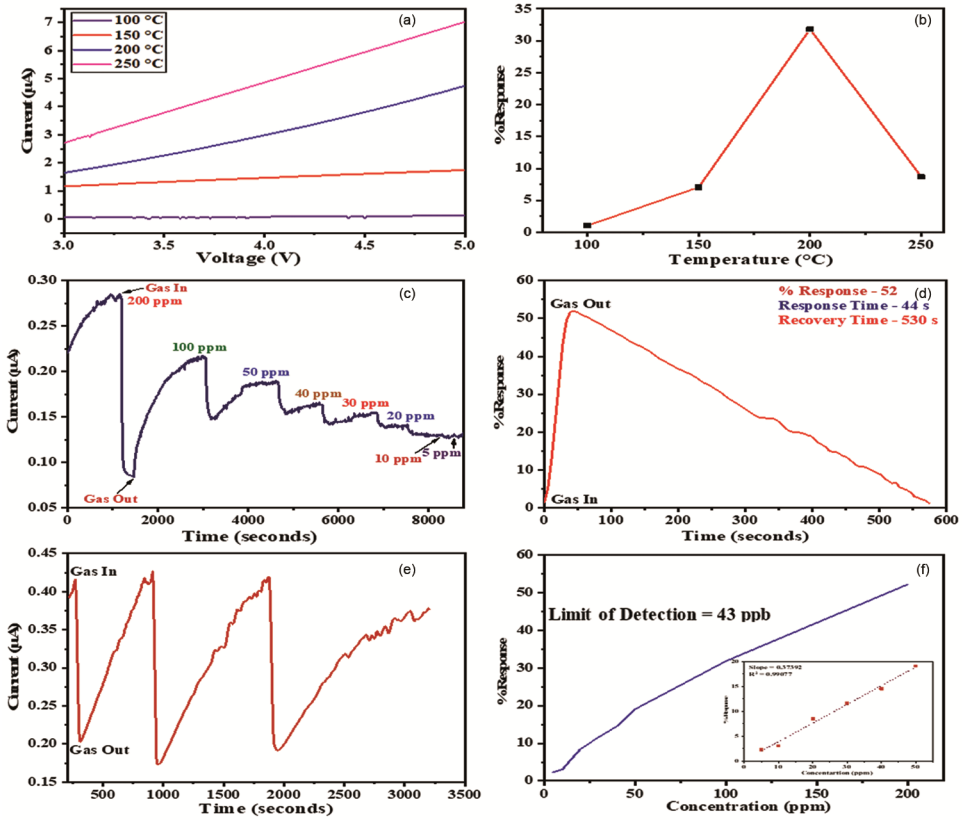

Fig. 3 — (a) I-V characteristics at different temperatures (b) % Responsivity towards 100 ppm of NO_2 at varying temperatures (c) Dynamic variation in current with different concentration of NO_2 (d) Response curve of NO_2 gas sensor at concentration of 200 ppm (e) Repeatability cycle for 200 ppm concentration and (f) Variation in % Response with different concentration of NO_2, linear fit data (inset Figure)

of total 200 sccm which is controlled by two mass flow controllers (MFC) connected to the system. The gas sensing analysis of the prepared film was done at different temperatures and the relative humidity range of 35%. Initially, air was inserted in the chamber and corresponding value of current is noted down. After that, the required amount of gas analytes was inserted in the chamber by keeping total flow rate constant. The insertion of gas analytes decrease the current value from its baseline value and thus the decrement is noted further. The concentration of the gas analytes was calculated using the following Eq. 2,

$$\text{Desired concentartion (in ppm)} = \frac{\text{Flow rate (in sccm) of gas analytes}}{\text{Total flow rate (in sccm)}} \times \text{ppm of gas analytes cylinder} \quad \ldots (2)$$

Figure 3 emphasizes the sensing analysis of ZnO film for NO_2 gas corresponding to different temperatures. The defects present in the film facilitate the adsorption of NO_2 gas species onto the film surface, resulting in better response for the sensor.

Initially, the I-V characteristics of the developed film were examined at various temperatures, illustrated in Fig. 3(a). The I-V curve represented the ohmic behaviour when the film is operated in the voltage region of 3 to 5 V, providing a good and stable electric contact between the electrode and sensor. The increase in the current value indicated that the fabricated film is semiconducting in nature, which makes it suitable for chemiresistive gas sensors. The gas sensing analysis of the film was carried out at a constant voltage of 4V. The corresponding percentage response was calculated using the following formula (Eq 3),

$$R\% = \frac{|I_a - I_g|}{I_a} \times 100 \quad \ldots (3)$$

Here, I_a and I_g, respectively, represent the current value in air and the environment of sensing gas.

The operating temperature is an important parameter which affects the sensing performance of the gas sensor as variation in temperature result in different sensing response, response and recovery

Table 1 — Summary of metal-oxide based fabricated sensor via sputtering for detection of NO_2

Sr. No.	Material	Substrate	Substrate Temperature (℃)	Power	Operating Temperature (℃)	Concentration	Response	References
1.	WO_3/Si	-	-		250	100 ppm	22.7%	[24]
2.	ZnO	Si	RT	60 W	250	20 ppm	29.2%	[25]
3.	Ag−WO_{3-x}	Si/SiO_2	500	40 W	225	10 ppm	70%	[26]
4.	ZnO	Glass	RT	25 W	200	200 ppm	52%	This work

time. Therefore, the sensing analysis was performed at different temperatures ranging from 100 to 250 ℃ for 100 ppm concentration of NO_2 (Fig. 3 (b)). The response was obtained highest in case of film operated at temperature 200 ℃. All the analysis was performed at operating temperature of 200℃. Fig. 3 (c) represents the sensing response curve for ZnO film at varying concentrations of NO_2 gas ranging from 5 ppm to 200 ppm. It was observed that the response increased from 3% to 20% for an increase in concentration from 5 to 100 ppm. At 200 ppm concentration, the sensor showed maximum response (approx. 52%). This showed the good interaction capability of the sensor with the analyte gas, which is related to the exposed area of the sensing element, i.e., the greater the exposed area, the greater the interaction capability of the sensor with the sensing gases.

The recovery time of a gas sensor is defined as the time elapsed to achieve 90 % of maximum response upon exposure of the analyte gas, while recovery time is the time required to return to 10 % of its initial value after removal of the analyte gas. When ZnO sensor was exposed to the target gas (NO_2 gas) then the sensor showed a decrease in the value of current and with the removal of gas, it showed an increment in the current value. Fig. 3(d), emphasized the rapid response dynamics of the sensor, but the slowly decreasing current rate result in the slow recovery. So, ZnO sensor exhibited high adsorption rate and chemical sensing reaction mechanism, but on the other hand, the desorption rate was slow that resulting in slow recovery. The response curves shown in Fig. 3(d) represent the time duration for response and recovery of the sensor in NO_2 atmosphere, which is 44 s and 530 s, respectively.

The repeatability was tested for a 200 ppm of analyte gas shown in Fig. 3(e). This shows that the sensor exhibits good recyclability for the ZnO sensor. The percentage response vs concentration data plot is shown in Fig. 3 (f). The inset Figure represents the linear fitting of the curve, with R^2 and slope values are 0.99077 and 0.37392, respectively. The detection limit of the sensor was calculated using Eq. (4), provided by the IUPAC standard,

$$Limit\ of\ Detection\ (LOD) = 3 \times \frac{noise_{rms}}{S} \quad \ldots (4)$$

where, the terms $noise_{rms}$ and S, respectively, are the root mean square value of noise in the signal and sensitivity given by slope of inset Fig. 3 (f). The noise in the signal can be computed by Eq. (5),

$$noise_{rms} = \sqrt{\frac{\sum(I_O - I_C)^2}{N}} \quad \ldots (5)$$

where, I_O and I_C respectively represents the observed and calculated current, computed by fitting the 5th-order polynomial of 26 consecutive data point set on the baseline curve of current. The estimated value from Eq. (5) was 0.0054. Based on the above data, the detection limit calculated from Eq. (4) was found to be 43 ppb for the present sensing film[22,23]. The present study comprises cost effective approach utilizing glass substrate with low power and low operating temperature compared with previous studies and the results are summarized in Table 1.

5 Sensing Mechanism

The mechanism behind the materials sensing using chemiresistive gas sensor involves the change in value of electrical current, which was basically due to the adsorption-desorption process of oxygen species during the interaction between the interface of gas analytes and adsorbed oxygen. In presence of air, the oxygen molecules get adsorbed onto the sensing material surface and make the material electron deficient by extracting conduction band electrons. The species formed on the material surface depend on the temperature at which the material senses, it takes the form O_2^-, O^- and O^{2-} if the operating temperature is less than 100 ℃, between 100-300 ℃ and above 300 ℃, respectively[27,28,29].

$$O_2(gas) \leftrightarrow O_2(absorbed)$$

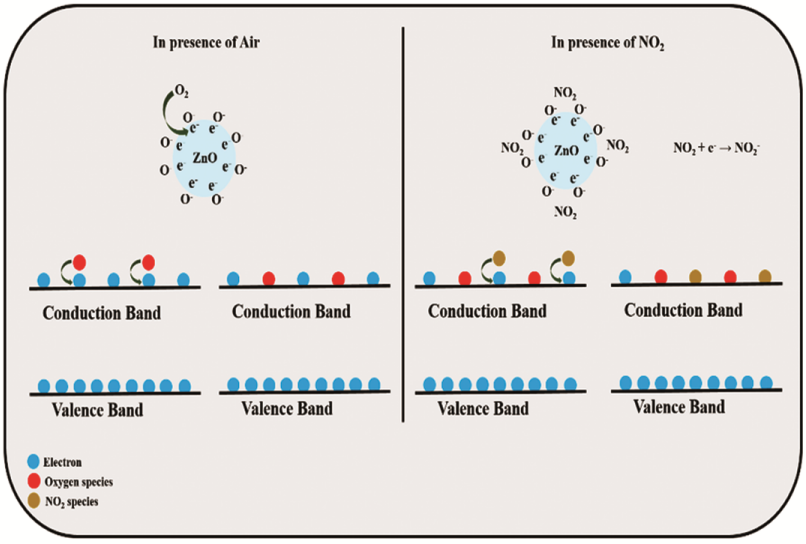

Fig. 4 — Schematic representation of gas sensing mechanism of ZnO for NO_2 gas

$$O_2(absorbed) + e^- \leftrightarrow O_2^-(< 100\ ℃)$$
$$O_2^- + e^- \leftrightarrow 2O^-(100 - 300\ ℃)$$
$$O^- + e^- \leftrightarrow O^{2-}(> 300\ ℃)$$

The sensing performance depends on many parameters like adsorption or desorption rate, oxygen vacancies, oxidizing or reducing character of sensing gas, operating temperature, etc.

The prepared ZnO film was n-type (electrons are the majority charge carriers) in nature. When ZnO film was subjected to air, the adsorption of oxygen molecules onto the film surface occurred, forming the depletion layer on the surface. This depletion layer generally decreases the current value of the sensor, but in our case, the effects of an increase in temperature dominated, thus the overall effect of air and temperature showed an increment in the current value (Fig. 3 (c)). On the other hand, when the film exposed to oxidizing gas (i.e., NO_2), the gas species further extracted the conduction band electrons and thus participated in enhancing the depletion layer further. This enhancement of the depletion layer reduced the current value by overcoming the effect of temperature[23]. The mechanism for ZnO sensor corresponding to NO_2 gas is provided in Fig. 4.

6 Conclusion

ZnO thin film sensor is developed by the DC magnetron sputtering technique on a glass substrate. The sputtered ZnO nano structured film showed good response for NO_2as an analyte gas. The operating temperature for the sensing element was 200 ℃. It exhibited a high response of 52 % for a 200 ppm concentration of NO_2. The sensor was also suitable for detecting the lower concentrations upto 5 ppm of analyte gas, achieving a response value of 3%. The sensor had good consistency in its behavior with a response and recovery time of 44 s and 530 s, respectively, and having good detection limit of 43 ppb. Therefore, this study shows that the fabricated film sensing element exhibits better stability, good response and recovery time and reliable repeatability for concentrations of 5 to 200 ppm of the analyte gas.

References

1 Shaba E Y, Jacob J O, Tijani J O & Suleiman M A T, *Appl Water Sci*, 11 (2021) 48.
2 Das S, Mojumder S, Saha D & Pal M, *Sens Actuators B Chemi*, 352 (2022) 131066.
3 Shen Y, Liu Y, Fan C, Wang Q, Li M, Yang Z & Gao L, *Sensors*, 24 (2024) 2110.
4 Khudiar S S, Nayef U M, Mutlak F A H & Abdulridha S K, *Optik,* 249 (2022) 168300.
5 Umar A, Akbar S, Kumar R, Amu-Darko J N O, Hussain S, Ibrahim A A & Seliem A F, *Chemosphere,* 349 (2024) 140838.
6 Komorizono A A, Leite R R, De la Flor S, Llobet E & Mastelaro V R, *Mater Sci Semiconduct Process,* 188 (2025) 109229.
7 Kumar S, Betal A, Kumar A, Chakkar A G, Kumar P, Kwoka M, Sahu S & Kumar M, *ACS Sensors,* 10 (2025) 2191.
8 Huang H, Pan Z, Wang J, Wang T, Yang W, Yu H, Li F, Dong X & Yang Y, *Sens Actuators B Chemi,* 433 (2025) 137569.
9 Zhu C, Lv T, Yang H, Li X, Wang X, Guo X, Xie C & Zeng D, *Mater Today Comm*, 34 (2023) 105116.
10 Lv J, Zhang C, Qu G, Pan K, Qin J, Wei K & Liang Y, *Talanta*, 273 (2024) 125853.
11 Khomarloo N, Mohsenzadeh E, Gidik H, Bagherzadeh R & Latifi M,*RSC Advances*, 14 (2024) 7806.

12 Berwal P, Sihag S, Rani S, Kumar A, Jatrana A, Singh P, Dahiya R, Kumar A, Dhillon A, Sanger A, Kumar M, Sharma A & Kumar V, *Ind Eng Chem Res*, 62 (2023) 14835.
13 Kumar V, Kumar A, Priyanka, Sihag S & Jatrana A, *Handbook of Green and Sustainable Nanotechnology*, (2022) 1.
14 Rani S, Dahiya R, Kumar V, Berwal P & Sihag S, *Ionics*, 31(2024) 1.
15 Sihag S, Dahiya R, Rani S, Berwal P, Jatrana A, Kumar A & Kumar V, *Appl Phys AMater Sci Process*, 129 (2023) 1.
16 Kannan P K, Saraswathi R & Rayappan J B B, *Ceramics Int*, 40 (2014) 13115.
17 Hassan M M, Khan W, Mishra P, Islam S S & Naqvi A H, *Mater Res Bullet*, 93 (2017) 391.
18 Wang G, Chen T, Guo L, Wang H, Wang X, Zeng H, Feng Y, Zhao W, Wang Y, Liu X, Wang J & Yang Y, *Sens Actuators B Chem,* 413 (2024) 135862.
19 Xavier R & Sivaperuman K, *Mater Today Comm,* 38 (2024) 107831.
20 Abdelghani G M, Ahmed A B & Al-Zubaidi A B, *Sci Rep*, 12 (2022) 20016.
21 Dulta K, Koşarsoy Ağçeli G, Chauhan P, Jasrotia R & Chauhan P K, *J Cluster Sci,* 33 (2022) 1.
22 Sheokand A, Kumar V, Sindhu S, Bulla M, Dahiya R & Jatrana A, *Sens Actuators A Phys*, 382 (2025) 116121.
23 Pan Z, Huang H, Wang T, Yu H, Yang W, Dong X & Yang Y, *Talanta,* 294 (2025) 128194.
24 Singh S, Gurawal P, Malik G, Adalati R, Kaur D & Chandra R, *Micro Nanostruct,* 188 (2024) 207794.
25 Varshney P, Kumar V, Singh P, Sharma R & Kumar A, *J Phys Sci,* 33 (2022) 1.
26 Hossain M, Sarkar K, Mondal A, Bag A, Kuiri P K, Roopa Kumar M S, Bysakh S & Pal P, *Appl Phys A Mater Sci Process*, 129 (2023) 1.
27 Sihag S, Dahiya R, Rani S, Berwal P, Jatrana A, Sisodiya A K, Sharma A & Kumar V, *Discover Nano*, 19 (2024) 1.
28 Yan Y, Xu J, Peng Z, Ji Z, Gao Y, Jia L & Xu Q, *Electron,* 13 (2024) 4800.
29 Goyal D, Goyal C P, Chidambaram D, Sivalingam Y, Ikeda H, Ponnusamy S & Ramgir N S, *J Mater Sci Mater, Electron,* 35 (2024) 960.